Journal of Industrial and Management Optimization

https://www.aimspress.com/journal/jimo

JIMO, 22(4): 2119–2146.
DOI:10.3934/jimo.2026078
Received: 26 December 2025
Revised: 17 March 2026
Accepted: 24 March 2026
Published: 28 March 2026

Research article

A lattice partition-based approach for critical states identification in a power system

Feiyu Chen[1], Han Hu[1], Wenjie Wan[1], Hongyu Zhang[1], Xiaoyu Liu[1,*], Bo Yu[1] and Kequan Zhao[2]

[1] National Center for Applied Mathematics in Chongqing, Chongqing Normal University, Chongqing, China

[2] School of Mathematical Sciences, Chongqing Normal University, Chongqing, China

* **Correspondence:** Email: xyliu@cqnu.edu.cn.

Abstract: Critical states in power systems, also known as minimum cut sets, are core to quantifying reliability risks as they directly reflect the weakest links causing system failures. Existing methods either fail to comprehensively capture all critical states or suffer from excessive computational complexity, hindering efficient reliability assessment. To address these issues, this paper proposed a lattice partition-based critical states identification (LPCSI) method to identify all critical states up to a preset level and accelerate reliability assessment. First, a mathematical lattice structure was employed to represent and partition the power system state space. Leveraging system coherence, the method directly identifies numerous high-level failure states via lattice partition and simple state comparison, instead of time-consuming optimal power flow(OPF) calculations, enabling efficient critical state identification. Meanwhile, the probability of these high-level failure states is computed using a simple formula based on lattice properties, simplifying reliability index calculation, allowing monotonic convergence to the upper and lower bounds of the loss of load probability (LOLP). Experiments on the Roy Billinton test system (RBTS) and the IEEE reliability test system 1979 (RTS79) demonstrate that the proposed method accurately identifies all preset-order critical states (high-risk states). Compared to traditional methods like state enumeration (SE) and Monte Carlo simulation (MCS), the LPCSI method offers superior accuracy and efficiency in reliability assessment.

Keywords: optimization of reliability assessment; power system reliability; critical states; lattice partition; state extension
Mathematics Subject Classification: 90C06, 90C90, 60K05, 06B99

1. Introduction

With the development of power systems toward ultra-high voltage, long-distance transmission, and large capacity, various reliability assessment methods have been developed, including those using failure prediction, maintenance optimization, and intelligent algorithms for floating offshore wind turbine components [1, 2], network cooperation recovery or distributed communication for system reliability enhancement and evaluation [3, 4], and analytical approaches considering time-varying component failure rates [5]. Besides, precisely identifying minimal cut sets (critical states) can provide better insights into the power system's vulnerabilities [6], which not only helps assess the reliability of existing systems but also provides important theoretical foundations for enhancing system stability and robustness [7–9].

The minimum cut set method has been widely applied for fault analysis and system optimization [10,11]. Traditional methods include fault tree analysis (FTA) [12, 13], and network-based analysis methods, such as the max-flow min-cut theorem [14, 15] and the minimum cut set-network equivalence method [16], which were proposed to determine minimum cut sets and assess system reliability. However, the above methods either struggle with dynamic scenarios or primarily rely on topological structures, which leads to either missed important cut sets or redundant results.

When combined with optimal power flow (OPF) analysis, monte carlo simulation (MCS) methods and state enumeration (SE) can also be employed to identify minimal cut sets [7, 16]. These methods can provide more accurate evaluations by considering both system topology and operational constraints. However, MCS for identifying minimum cut sets is inefficient due to its need for extensive simulations and may overlook rare or low-probability cut sets. SE suffers from exponential computational complexity, making it impractical for large-scale systems. To improve that, methods like Markov minimal cut sets [17], fast sorting algorithm(FSAs) [18, 19], a bi-level optimization model [20], and a state selection technique [21] are proposed to reduce the number of system states and identify some high-risk system states. But these methods fail to determine minimal cut sets completely and accurately in large-scale systems.

Based on system coherence, some other methods like system state space classification [22], state extension based on tree structure [23, 24], and impact increment SE [25] are proposed to perform state extension, which consider the effects of high-level failure states by only evaluating low-level states to achieve higher indices within a limited number of evaluations. However, some of these methods have limited state extension areas, and those capable of identifying minimum cut sets all calculate the indices based on the inclusion-exclusion principle, which is computationally intensive and provides only fuzzy upper and lower bounds.

To address these issues, this paper applied a mathematical structure-a lattice-the partial order property of which shares certain commonalities with system coherence [26]. Therefore, it can serve as a state extension tool to consider the effects of high-level failure states. Reliability assessment will benefit from lattice structure in three aspects: 1) reducing the number of OPF calculations by expanding the state extension area, which overcomes the limitation of a limited extension area in [23]; 2) enabling flexible partition of the entire system space into non-overlapping lattices, which addresses the drawback of inefficiently calculating indices using the inclusion-exclusion principle due to an overlapping state extension area in [17]; 3) allowing the sum of probabilities of many high-level failure system states to be calculated using a simple formula, thanks to the property of the lattice structure. Meanwhile, it enables the critical system states identification to be conducted in a comprehensive and efficient manner.

(Critical states are states where only components in minimal cut sets have failed.) The proposed method partitions the system state space into lattices in a recursive way so that critical system states can be fully and efficiently identified up to a preset level by successive evaluation and comparison, which provides a new and effective solution for power system reliability assessment. In summary, the main contributions are as follows:

1. Based on the system coherence assumption, the definition and properties of critical system states are clearly clarified, and a Boolean lattice structure representation method for the system state space is proposed, which enables effective extension of the knowledge of the evaluated system states to include the effects of unevaluated high-level states.

2. An efficient critical state identification method is developed, which can simultaneously perform lattice partition of the system state space. In addition, the contribution of critical states to the LOLP can be quantified.

3. Based on the identified critical system states and lattice partition results, a lattice-based calculation method for the reliability index LOLP is proposed. This method eliminates the need for a large number of OPF calculations, and the upper and lower bounds of the LOLP can be monotonically derived with progressive convergence.

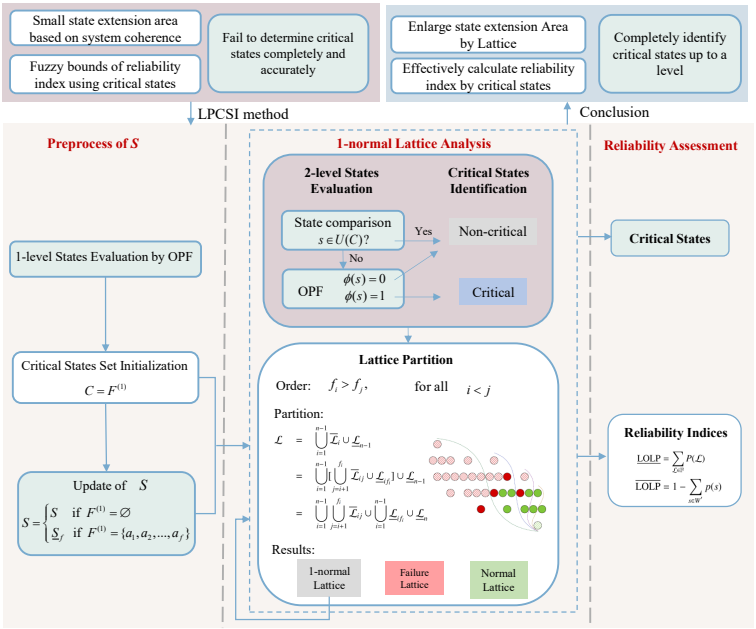

Figure 1. Research framework of the proposed method.

The framework of the proposed method is shown in Figure 1 and this paper is organized as follows: Section 2 illustrates the mathematical representation of system states and defines the critical states; Section 3 gives the definition of a lattice in the state space and proposes an approach to partition the state space into lattices by 1-level states and 2-level states; Section 4 analyses 1-normal lattices, gives the algorithm for identifying critical states in a 1-normal lattice, gives the overall process of the proposed method, Lattice based Critical States Identification(LPCSI), to determine the critical states and calculate

the LOLP index of a system; and Section 5 conducts experiments on the RBTS and RTS-79 systems, proving the efficiency of the method.

2. Structure analysis of the state space of the power system

2.1. Basic concepts of the power system states

Assume a composite power system contains n components numbered sequentially $1, 2, ..., n$, and a component is considered either operational or failed in our study. Then a system state can be represented as the set of its failed components. For example, a system state $s \in S$ with k failed components is represented as $s = \{i_1, i_2, \ldots, i_k\}$, where components $i_1, i_2, \ldots, i_k$ have failed, and the others are operational. In particular, $\hat{0} = \{\}$ represents the system state where all components are operational, and $\hat{1} = \{1, 2, ..., n\}$ represents the state in which all components have failed. The term *state* as used in the following discussion will imply a system state. The state space of the power system is denoted by S, which contains 2^n states.

Definition 2.1. *A k-level state is defined as a state with k failed components.*

The level of s is denoted as $\rho(s)$. In particular, $\hat{0} = \{\}$ is a 0-level state and $\hat{1} = \{1, 2, ..., n\}$ is an n-level state. For example, for a 5-component system, $s = \{1, 3, 5\}$ is a 3-level state where components 1, 3, 5 are failed, components 2, 4 are operational, and $\rho(s) = 3$.

Definition 2.2. *Failure states are defined as states where load shedding occurs, while normal states are defined as states where no load shedding occurs. The terms* failure *and* normal *are referred to as the statuses of a state.*

The load shedding of a state s is represented as $C(s)$ and is determined using the DC optimal power flow model (OPF), which can give a good approximation of active power flows in power systems:
Objective function:

$$C(s) = \min \sum_{i \in N_D} P_{Ci} \tag{1}$$

Constraints:

$$\begin{gathered} B\Theta + P_G + P_C = P_D \\ 0 \le P_G \le P_G^{\max} \\ 0 \le P_{Ci} \le P_{Di} \\ |T(s)| \le T^{\max} \end{gathered} \tag{2}$$

where P_{Ci} is the load shedding of node i and $C(s)$ is the total load shedding amount, B is the nodal admittance matrix, Θ is the voltage phase angle vector, and P_G, P_C, and P_D are the node generator active power injection vector, node load reduction vector, and node active load vector, respectively. $T(s)$ is the active power vector of the lines in state s. $P_G^{\max}$ and $T^{\max}$ are the upper limit of generator output and the maximum capacity of branch power flow, respectively.

Definition 2.3. *Define a function on the system state space as* $\Phi : S \to \{0, 1\}$*:*

$$\Phi(s) = \begin{cases} 0 & s \text{ is a normal state} \\ 1 & s \text{ is a failure state} \end{cases} \tag{3}$$

Definition 2.4. *The failure and the normal state space of* S *are defined as* F *and* N*:*

$$F = \{s \in S \mid \Phi(s) = 1\}; \quad N = \{s \in S \mid \Phi(s) = 0\} \tag{4}$$

For convenience, we denote the set of all the k-level states in $T \subseteq S$ as $T^{(k)}$ in the following discussion. For example, $F^{(k)}$ is the set of all the k-level failure states in S.

2.2. Critical state

Definition 2.5. *For any* $s, t \in S$*, if* $s \subseteq t$*, we say that* s *is less than or equal to* t*, denoted as* $s \leq t$*. Equivalently,* t *is greater than or equal to* s*, denoted as* $t \geq s$*.*

For example, $\{1, 3, 5\} < \{1, 3, 4, 5\}$ and $\{2, 3, 5\} > \{3, 5\}$. In fact, the relation "$\leq$" in S is a partial order as defined in [26]. Therefore, we can establish the following proposition:

Proposition 2.1. $(S, \leq)$ *is a partially ordered set, where for any* $s \in S$*,*

$$\{\} = \hat{0} \leq s \leq \hat{1} = \{1, 2, \ldots, n\} \tag{5}$$

Here, $\hat{0} = \{\}$ *is the minimum element of* S *and* $\hat{1} = \{1, 2, \ldots, n\}$ *is the maximum element of* S*.*

System coherence is the basic assumption of reliability evaluation of a composite power system in this paper. System coherence implies that the system performance could not get better if an operational component fails, and not get worse if a failed component is repaired. This property holds in most complex power systems, especially in high-level failure states [23]. Although strict coherence might be difficult to guarantee in practice, such non-coherent scenarios are relatively rare, and their impact on reliability evaluation is minor. Thus, on the assumption of general system coherence, the following proposition can be established.

Proposition 2.2. *Assume* $s \in S$ *and* $t \leq s$*. Then:*

1. *If* $\Phi(t) = 1$*, then* $\Phi(s) = 1$*.*
2. *If* $\Phi(s) = 0$*, then* $\Phi(t) = 0$*.*

Since $t \leq s$ indicates that there are more failed components in s than in t, if t is a failure state ($\Phi(t) = 1$), then s with more failed components must also be a failure state; conversely, if s is a normal state ($\Phi(s) = 0$), then t with less failed components must also be normal ($\Phi(t) = 0$). The first case in Proposition 2.2 refers to the extension of failure status from state t to s, which we call *state extension*, which is consistent with the concept in [24].

Definition 2.6. *A state* $c \in S$ *is defined as a critical state if and only if* $\Phi(c) = 1$ *and* $\Phi(s) = 0$ *for all* $s < c$*.*

By Definition 2.6, a critical state c has failed, yet any state $s < c$ remains normal. Thus, c sits precisely at the threshold where the system transitions from normal to failed. Therefore, critical states refer to those lying on the boundary between the normal state space and the failure state space, from which the term "critical state" derives its name. The set of all the critical states is denoted as C. According to Proposition 2.2, states greater than a critical state are definitely failure states. In fact, a failure state is either a critical state or is greater than a critical state, and the following proposition is established.

Proposition 2.3. *If $C \subset S$ is the set of all the critical states in S, then*

$$C \cup U(C) = F \tag{6}$$

where $U(C) = \{s \in S \mid s > c, \exists c \in C\}$ denotes all the states greater than at least one state in C.

In critical states, the failure of an additional component leads to system outage, while repairing a failed component restores the system to normal operation. Specifically, a critical system state refers to the condition where all components in the corresponding minimal cut set have failed. Under the premise of system coherence, "critical state" and "minimal cut set" are essentially equivalent: the former describes the system operating condition, while the latter denotes the set of failed components; they both point to the same physical process of system failure caused by the weakest link, differing only in the naming perspective. In this paper, we focus on system state analysis, hence the term "critical state" is proposed and adopted. In Section 3, we introduce an important concept of a Boolean lattice, which helps with critical states identification and reliability calculation.

2.3. Boolean lattice representation of the system state space

Definition 2.7. *A lower bound for $s, t \in S$ is an element $l \in S$ such that $l \leq s$ and $l \leq t$, and an upper bound for $s, t \in S$ is an element $u \in S$ such that $u \geq s$ and $u \geq t$.*

Definition 2.8. *s, t have a least upper bound or join if there is a state in S, denoted $s \vee t$, which is an upper bound for s, t and $s \vee t \leq u$ for all upper bounds u of s and t. Correspondingly, the greatest lower bound or meet of s and t is denoted as $s \wedge t$.*

The least upper bounds of all the states in a set T are denoted as $\vee(T)$. For example, $\{1, 3, 4, 5\} \wedge \{2, 3, 5\} = \{3, 5\}$, $\{2, 3, 5\} \vee \{1, 3, 5\} = \{1, 2, 3, 5\}$, $\vee(\{\{1, 2\}, \{1, 2, 5\}, \{4, 5\}\}) = \{1, 2, 4, 5\}$.

Definition 2.9. *A Boolean lattice $\mathcal{L}$ is a partially ordered set in which every element $x \in \mathcal{L}$ has a unique complement $\bar{x} \in \mathcal{L}$ such that $x \wedge \bar{x} = \hat{0}_{\mathcal{L}}$ and $x \vee \bar{x} = \hat{1}_{\mathcal{L}}$, where $\hat{0}_{\mathcal{L}}$ is the minimum element and $\hat{1}_{\mathcal{L}}$ is the maximum element of $\mathcal{L}$.*

Definition 2.10. *Assume $\bar{s}, \underline{s} \in S$, $\underline{s} \leq \bar{s}$, and then the corresponding closed interval is defined as $[\underline{s}, \bar{s}]$:*

$$[\underline{s}, \bar{s}] = \{s \in S \mid \underline{s} \leq s \leq \bar{s}\} \tag{7}$$

where $\underline{s}$ is the minimum element and $\bar{s}$ is the maximum element of the interval $[\underline{s}, \bar{s}]$.

Proposition 2.4. *An interval $[\underline{s}, \bar{s}]$ is a Boolean lattice.*

A Boolean lattice is presented by an interval in this paper. In particular, S is an n-dimensional Boolean lattice presented as $[\hat{0}, \hat{1}]$.

Definition 2.11. *Given a Boolean lattice $\mathcal{L} = [\underline{s}, \bar{s}] \subseteq S$, the dimension of $\mathcal{L}$ is defined as $D(\mathcal{L}) = \rho(\bar{s}) - \rho(\underline{s})$, and $\mathcal{L}$ can be called a $D(\mathcal{L})$-dimension Boolean lattice.*

In particular, if $\underline{s} = \bar{s}$, then $[\underline{s}, \bar{s}] = \{\underline{s}\}$, which is a 0-dimensional Boolean lattice and contains only one state.

In fact, a Boolean lattice can be seen as the state space of a system or a subsystem. For example, the state space of a 5-component system can be represented by the 5-dimensional Boolean lattice $S = [\{\}, \{1, 2, 3, 4, 5\}]$, and the 3-dimensional sublattice $\mathcal{L} = [\{1, 3\}, \{1, 2, 3, 4, 5\}]$ is the state space of a 3-component system, where components 1 and 3 are fixed as failed. The Hasse diagram of the lattice $\mathcal{L}$ is shown in Figure 2.

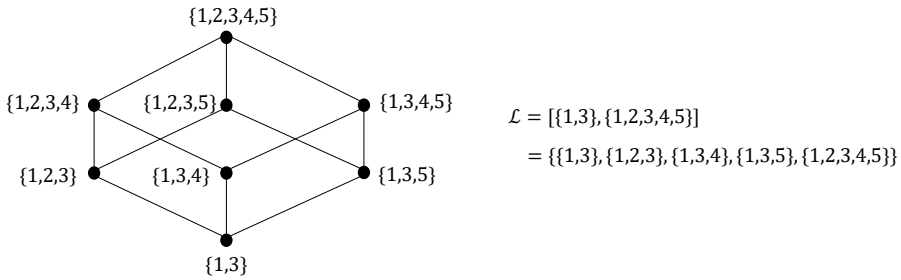

Figure 2. A Boolean lattice in S.

Moreover, consider the state $\{1, 2, 3, 5\}$, where its level in the original lattice (the state space of the system) is $\rho(\{1, 2, 3, 5\}) = 4$, while $\rho_{\mathcal{L}}(\{1, 2, 3, 5\}) = \rho(\{1, 2, 3, 5\}) - \rho(\{1, 3\}) = 4 - 2 = 2$. Thus, $\{1, 2, 3, 5\}$ is a 4-level state in S, and also a 2-level state in $\mathcal{L}$. The term *lattice* as used in further discussions will imply a Boolean lattice. Two special types of lattices are introduced as follows.

Definition 2.12. *A k-normal lattice is defined as a lattice in which all k-level states are normal.*

Definition 2.13. *A failure lattice is defined as a lattice whose minimum element is a failure state.*

It is noted that a 1-normal lattice is also a 0-normal lattice according to Proposition 2.2. All states in a failure lattice are failure states, as they are greater than or equal to the minimum failure state; therefore, a failure lattice cannot be a k-normal lattice. Based on the fact that any state strictly less than a critical state must be a normal state, an important property is established as follows.

Property 2.1. *In a failure lattice, only the minimum element may be a critical state.*

According to Property 2.1, if failure lattices can be partitioned out from S, the OPF calculations and comparisons between states will be reduced when searching for critical states, since only the minimum elements of the failure lattices need to be considered. Thus, Section 3 proposes a basic strategy to partition out failure lattices from S.

3. Lattice partition of the state space of the power system

Before illustrating the lattice partition, some notations in a lattice $\mathcal{L}$ are introduced.

Let $\mathcal{L}$ be the state space of an n-component system state space with ordered 1-level states, where the 1-level states and 2-level states of $\mathcal{L}$ are denoted as

$$a_i = \{i\} \qquad \text{for } 1 \le i \le n \tag{8}$$

$$a_{ij} = \{i, j\} \quad \text{for } 1 \le i < j \le n \tag{9}$$

The corresponding conjugate states of a_i and a_{ij} are denotes as:

$$t_i = \vee(\{a_k\}_{k=i}^{n}) \quad \text{for } 1 \le i \le n \tag{10}$$

$$t_{ij} = \vee(\{a_{ik}\}_{k=j}^{n}) \quad \text{for } 1 \le i < j \le n \tag{11}$$

In particular, we set $a_0 = t_{n+1} = \hat{0}_{\mathcal{L}}, t_{i(n+1)} = a_i$.
For a 5-dimension lattice, the above notations are shown in Figure 3(a).

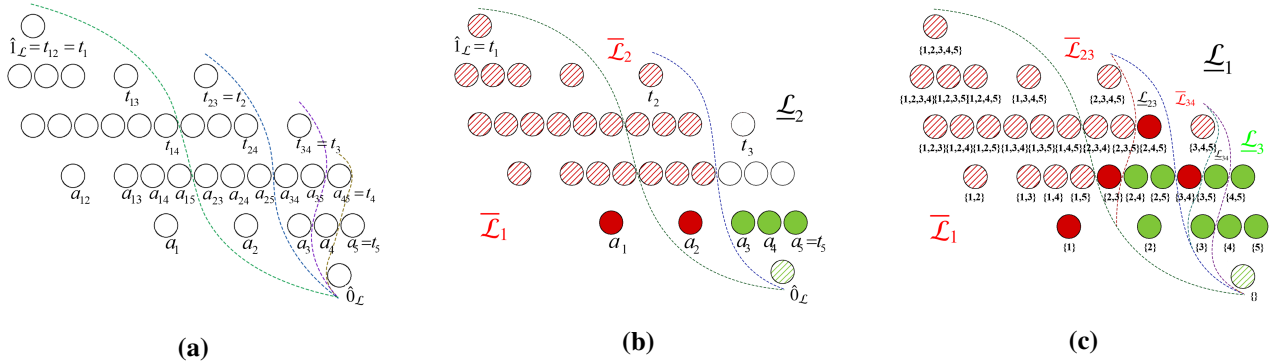

Figure 3. Labeling and an example of a partition of a 5-dimension lattice.
Note: Solid red circles denote the failure states evaluated by OPF, i.e., the critical states; solid green circles denote the normal states evaluated by OPF; and red shaded circles represent ordinary failure states (greater than the critical state).

3.1. Partition of lattice by 1-level states

Theorem 3.1. *Let $\mathcal{L}$ be an n-dimensional lattice with ordered 1-level states $\{a_1, a_2, ..., a_n\}$, and then $\mathcal{L}$ can be partitioned into $m + 1$ lattices:*

$$\mathcal{L} = \bigcup_{i=1}^{m} \overline{\mathcal{L}}_i \cup \underline{\mathcal{L}}_m \quad \textit{for } 1 \le m \le n \tag{12}$$

where

$$\overline{\mathcal{L}}_i = [a_i, t_i], \quad \underline{\mathcal{L}}_m = [\hat{0}_{\mathcal{L}}, t_{m+1}] \tag{13}$$

The partition result is not unique due to the different order of 1-level states.

Corollary 3.1. *If the 1-level states are ordered such that $\{a_1, a_2, ..., a_f\}$ are all the 1-level failure states, then each $\overline{\mathcal{L}}_i$ in (12) is a failure lattice, and $\underline{\mathcal{L}}_m$ in (12) is a 1-normal lattice.*

If $\mathcal{L}$ is an n-dimensional lattice containing $f < n$ failure 1-level states, then $\mathcal{L}$ can be partitioned into f failure lattices and one 1-normal lattice according to Corollary 3.1.

3.2. Partition of lattice by 1-level and 2-level states

Theorem 3.2. *Let $\mathcal{L}$ be an n-dimensional 1-normal lattice ($n \ge 2$) with ordered 1-level states $\{a_1, a_2, ..., a_n\}$. $\mathcal{L}$ can be partitioned as follows:*

$$\begin{aligned}\mathcal{L} &= \bigcup_{i=1}^{n-1} \overline{\mathcal{L}}_i \cup \underline{\mathcal{L}}_{n-1} \\ &= \bigcup_{i=1}^{n-1} [\bigcup_{j=i+1}^{f_i} \overline{\mathcal{L}}_{ij} \cup \underline{\mathcal{L}}_{if_i}] \cup \underline{\mathcal{L}}_{n-1} \\ &= \bigcup_{i=1}^{n-1} \bigcup_{j=i+1}^{f_i} \overline{\mathcal{L}}_{ij} \cup \bigcup_{i=1}^{n-1} \underline{\mathcal{L}}_{if_i} \cup \underline{\mathcal{L}}_{n-1} \\ &\quad \text{for } i+1 \le f_i \le n\end{aligned} \tag{14}$$

where

$$\overline{\mathcal{L}}_i = [a_i, t_i], \qquad \underline{\mathcal{L}}_i = [\hat{0}_{\mathcal{L}}, t_{i+1}], \tag{15}$$

$$\overline{\mathcal{L}}_{ij} = [a_{ij}, t_{ij}], \quad \underline{\mathcal{L}}_{ij} = [a_i, t_{i(j+1)}] \tag{16}$$

Corollary 3.2. *If the 1-level states are ordered such that* $\{a_{ii+1}, a_{ii+2}, \ldots, a_{if_i}\}$ *for* $i = 1, 2, \ldots, n-1$ *are all the failure 2-level states, then each* $\overline{\mathcal{L}}_{ij}$ *in (14) is a failure lattice.*

If $\mathcal{L}$ is a n-dimensional 1-normal lattice containing f 2-level failure states, then $\mathcal{L}$ can be partitioned into f failure lattices, $n-2$ 1-normal lattices, and one normal lattice according to Corollary3.2.

For example, consider the 5-dimension lattice $\mathcal{L} = [\{\}, \{1,2,3,4,5\}]$ with ordered 1-level states $\{\{1\},\{2\},\{3\},\{4\},\{5\}\}$, assume that 1-level states $\{1\}$ and $\{2\}$ have failed, then $\mathcal{L}$ can be partitioned into two failure lattices $\overline{\mathcal{L}}_1$ and $\overline{\mathcal{L}}_2$ and one 1-normal lattice $\underline{\mathcal{L}}_2$ based on Corollary 3.1:

$$\mathcal{L} = \overline{\mathcal{L}}_1 \cup \overline{\mathcal{L}}_2 \cup \underline{\mathcal{L}}_2 = [\{1\},\{1,2,3,4,5\}] \cup [\{2\},\{2,3,4,5\}] \cup [\{\},\{3,4,5\}]$$

which is shown in Figure 3(b). In another case, if only $\{1\}$ is the 1-level failure state, then $\mathcal{L}$ can be partitioned into $\overline{\mathcal{L}_1}$ and $\underline{\mathcal{L}}_1$, and $\underline{\mathcal{L}}_1 = [\{\},\{2,3,4,5\}]$ is a 4-dimension 1-normal lattice with ordered 1-level states $a_i = \{i+1\}$ for $i = 1, 2, \ldots, 4$, where we assume contains two 2-level failure states $\{2,3\}$ and $\{3,4\}$. Then $\underline{\mathcal{L}}_1$ can be partitioned into two failure lattices, two 1-normal lattices, and one normal lattice based on Corollary 3.2:

$$\begin{aligned}\mathcal{L} &= \overline{\mathcal{L}}_1 \cup \underline{\mathcal{L}}_1 \\ &= \overline{\mathcal{L}}_1 \cup \bigcup_{i=2}^{3} \bigcup_{j=i+1}^{f_i} \overline{\mathcal{L}}_{ij} \cup \bigcup_{i=2}^{3} \underline{\mathcal{L}}_{if_i} \cup \underline{\mathcal{L}}_3 \\ &= \overline{\mathcal{L}}_1 \cup \overline{\mathcal{L}}_{23} \cup \overline{\mathcal{L}}_{34} \cup \underline{\mathcal{L}}_{23} \cup \underline{\mathcal{L}}_{34} \cup \underline{\mathcal{L}}_3 \\ &= [\{1\},\{1,2,3,4,5\}] \cup [\{2,3\},\{2,3,4,5\}] \cup [\{3,4\},\{3,4,5\}] \\ &\quad \cup [\{2\},\{2,4,5\}] \cup [\{3\},\{3,5\}] \cup [\{\},\{4,5\}]\end{aligned}$$

which is shown in Figure 2(c).

4. Lattice partition-based critical states identification

4.1. Analysis of a 1-normal lattice

A 1-normal lattice can be divided into several failure sublattices and one lower-dimensional 1-normal sublattice depending on the status of 2-level states according to the above theorems and corollaries.

In general, the status of states are identified by OPF calculation, which is time-consuming for large-scale systems. Fortunately, the use of critical states, which are the minimum elements of the failure state space, is benefiting to reducing the number of OPF calculations.

$$s \in F \qquad \text{if } \Phi(s) = 1 \quad \text{or} \quad s \in U(\hat{C}) \tag{17}$$

where $\hat{C}$ is the current set of critical states and $\Phi(s)$ means the evaluation result of s by OPF.

The critical states should be identified by OPF calculations and level-by-level comparisons throughout the system space by definition. In fact, comparing with the current set of critical states is sufficient for critical state identification if the set of critical states is updated level-by-level.

$$s \in C \qquad \text{if } \Phi(s) = 1 \text{ and } \quad s \notin U(\hat{C}) \tag{18}$$

Based on formulas (17) and (18), we propose an efficient strategy for the identification of 2-level failure states and 2-level critical states in a 1-normal lattice.

Step 1: Judge the relationship between a 2-level state s and the current set of critical states $\hat{C}$:

$$s \in F \quad \text{but} \quad s \notin C; \qquad \text{if } s \in U(\hat{C}) \tag{19}$$

Step 2: Evaluate the status of s by OPF calculation if $s \notin U(\hat{C})$:

$$s \in F \quad \text{and} \quad s \in C; \qquad \text{if} \quad \Phi(s) = 1 \tag{20}$$

$$s \in N \quad \text{and} \quad s \notin C; \qquad \text{if} \quad \Phi(s) = 0 \tag{21}$$

After repeating the above two steps until the 2-level space $\mathcal{L}^{(2)}$ is traversed, all the 2-level failure states of the 1-normal lattice $\mathcal{L}$ are identified.

Denote f_i as the number of 2-level failed states of $\mathcal{L}$ contained in $\overline{\mathcal{L}}_i$, and $f = \sum_{i=1}^{n} f_i$ is the total number of 2-level failed states in $\mathcal{L}$. Clearly, f_i varies for different orders of components.

In order to partition out the failure lattices with a larger probability as much as possible, we reorder the components such that

$$f_i \geq f_j \qquad \text{for all} \quad i < j \tag{22}$$

In fact, condition (22) implements a "high-coverage-first" ordering strategy: components processed earlier correspond to higher-dimensional failure lattices $\overline{\mathcal{L}}_{ij}$ that contain more levels, collectively cover more failure states, and reduce the number of smaller 1-normal sublattices generated in subsequent partitions. This is essentially a greedy strategy: although it may not guarantee global optimality, it improves computational efficiency in practice.

For example, consider a 5-dimensional 1-normal lattice $\mathcal{L} = [\emptyset, \{1, 2, 3, 4, 5\}]$ with 2-level failure states $\{2, 3\}, \{2, 4\}, \{2, 5\}, \{3, 4\}$. Under the natural ordering $\{1, 2, 3, 4, 5\}$, component 1 appears in zero failure states yet is selected first. As shown in Figure 4(a), this yields a big 1-normal lattice $[\{1\}, \{1, 2, 3, 4, 5\}]$,

leaving all 11 states for recursive processing. In contrast, the proposed ordering $\{2, 3, 4, 5, 1\}$ prioritizes component 2, which appears in three failure states. The initial partition now covers four larger failure lattices than in natural order, leaving only two states in subsequent recursion, which is shown in Figure 4(b). In this case, the proposed ordering reduces the burden from 11 states to 2.

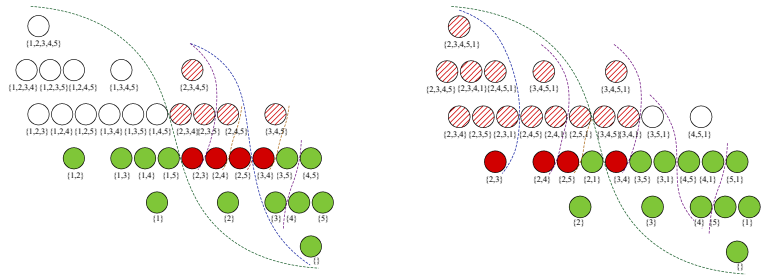

(a) **(b)**

Figure 4. Impact of component ordering on lattice partition efficiency.

Overall, the 1-normal lattice $\mathcal{L}$ can be partitioned according to Corollary 3.2, and the set of critical states is updated simultaneously. The whole procedure of analyzing a 1-normal lattice is described in the following algorithm:

Algorithm 1 1-normal lattice analysis algorithm

Input: A 1-normal lattice $\mathcal{L}$, the current set of critical states $\hat{C}$
Output: Updated $\hat{C}$, partition of $\mathcal{L}$
Begin
Initialize $\Phi(s) = 0$ for all $s \in \mathcal{L}^{(2)}$
for $s \in \mathcal{L}^{(2)}$ **do**
  if $s \in U(\hat{C})$ **then**
    $\Phi(s) = 1$
  else
    Evaluate s by OPF
    if s is a failure state **then**
      $\Phi(s) = 1$
      $\hat{C} = \hat{C} \cup \{s\}$
    end if
  end if
end for
Select the order such that (22) holds
Partition $\mathcal{L}$ by (14) with the above order
End

Note that the algorithm proposed to determine critical states is similar to the DC Optimal Power Flow Markov Cut-Set Method (DCOPF-MCSM) in [17] for identifying minimal cut sets, as both involve level-wise traversal comparing states against the current critical set and OPF evaluations. However, our method differs in two aspects: (i) rather than operating on the entire state space, LPCSI restricts these

operations to 1-normal lattices, significantly reducing the number of comparisons; (ii) the method in [17] requires complete identification of all critical states up to a certain level before reliability indices can be computed, whereas LPCSI enables incremental calculation of LOLP by accumulating probabilities of failure lattices during the identification process.

4.2. Reliability index calculation

Definition 4.1. *Define the probability function on the system state space as* $P : S \to [0, 1]$*:*

$$P(s) = \prod_{i \in s} p_i \prod_{i \notin s} q_i \tag{23}$$

where p_i *is the failed probability of component i,* q_i *is the operational probability of component i, and* $p_i + q_i = 1$.

Corollary 4.1. *Let a lattice be* $\mathcal{L} = [\underline{s}, \overline{s}]$*, and the probability of* $\mathcal{L}$ *is defined as the sum of probabilities of all the states in* $\mathcal{L}$*, which can be calculated by the following formula:*

$$P(\mathcal{L}) = P([\underline{s}, \overline{s}]) = \prod_{i \in \underline{s}} p_i \prod_{i \notin \overline{s}} q_i, \tag{24}$$

where p_i *and* q_i *are the failed probability and operational probability of component i, respectively.*

Since many failure lattices will be partitioned from the original lattice, LOLP of a system can be calculated as the sum of the probabilities of all the failure lattices. The lower and upper bounds of LOLP can be calculated as follows:

$$\underline{\text{LOLP}} = \sum_{\mathcal{L} \in \mathbb{F}} P(\mathcal{L}), \quad \overline{\text{LOLP}} = 1 - \sum_{s \in W'} p(s) \tag{25}$$

where $\mathbb{F}$ is the set of all the failure lattices partitioned out, W' is the set of normal states that have been evaluated by OPF, and the value of the $\underline{\text{LOLP}}$ is considered the final value of the LOLP for the power system reliability assessment of the proposed method. The following proposition establishes the monotonic convergence of these bounds to the true LOLP.

Proposition 4.1 (Monotonic convergence)**.** $\underline{\text{LOLP}}$ *is monotonically non-decreasing,* $\overline{\text{LOLP}}$ *is monotonically non-increasing, and both converge to the true value* LOLP_* *(the actual loss of load probability).*

Proof. Let $\mathbb{F}^{(t)}$ and $W'^{(t)}$ denote the sets of identified failure lattices and evaluated normal states at iteration t, respectively.

(1) Monotonicity. From (25), at iteration $t + 1$:

$$\underline{\text{LOLP}}^{(t+1)} = \underline{\text{LOLP}}^{(t)} + \sum_{\mathcal{L} \in \mathbb{F}^{(t+1)} \setminus \mathbb{F}^{(t)}} P(\mathcal{L}) \geq \underline{\text{LOLP}}^{(t)}, \tag{26}$$

$$\overline{\text{LOLP}}^{(t+1)} = \overline{\text{LOLP}}^{(t)} - \sum_{s \in W'^{(t+1)} \setminus W'^{(t)}} P(s) \leq \overline{\text{LOLP}}^{(t)}. \tag{27}$$

Thus, $\underline{\text{LOLP}}$ is non-decreasing and $\overline{\text{LOLP}}$ is non-increasing.

(2) Convergence. By construction, $0 \leq \underline{\text{LOLP}}^{(t)} \leq \text{LOLP}_* \leq \overline{\text{LOLP}}^{(t)} \leq 1$. By the monotone convergence theorem, both sequences converge. Since $\overline{\text{LOLP}}^{(t)} - \underline{\text{LOLP}}^{(t)} \to 0$ as $t \to \infty$, they converge to the same limit LOLP_*. □

4.3. Stop criteria

We set two stop criteria for the proposed approach:

1. Level (k): Level of states.
2. Gap between upper and lower bounds of LOLP (δ):

$$\delta = \overline{\text{LOLP}} - \underline{\text{LOLP}} \tag{28}$$

In fact, according to Proposition 4.1, the true value of the LOLP_* of the system lies within the interval defined by these two bounds. Thus, δ measures the interval range of the true LOLP value; smaller δ indicates a smaller interval, which indicates a more accurate assessment.

The algorithm is considered to have reached a certain level of precision when δ is less than the preset gap δ_* or all the states of the first k_* level have been searched, with k_* being the preset maximal level. The two stop criteria are also applicable to the SE method.

4.4. Process of the proposed approach

Let S be the state space of a given system. To identify the critical states of S and assess the reliability of the system, first, there is a preprocessing step: evaluate all the 1-level states in S by OPF and update S to a 1-normal lattice as follows:

$$S = \begin{cases} S & \textbf{if} \quad F^{(1)} = \emptyset \\ \underline{S}_f & \textbf{if} \quad F^{(1)} = \{a_1, a_2, ..., a_f\} \end{cases} \tag{29}$$

where f is the number of 1-level failure states in S, and $\underline{S}_f$ is the 1-normal lattice partitioned from S using (12). The overall process of the LPCSI method is shown in Figure 5 and elaborated as follows:

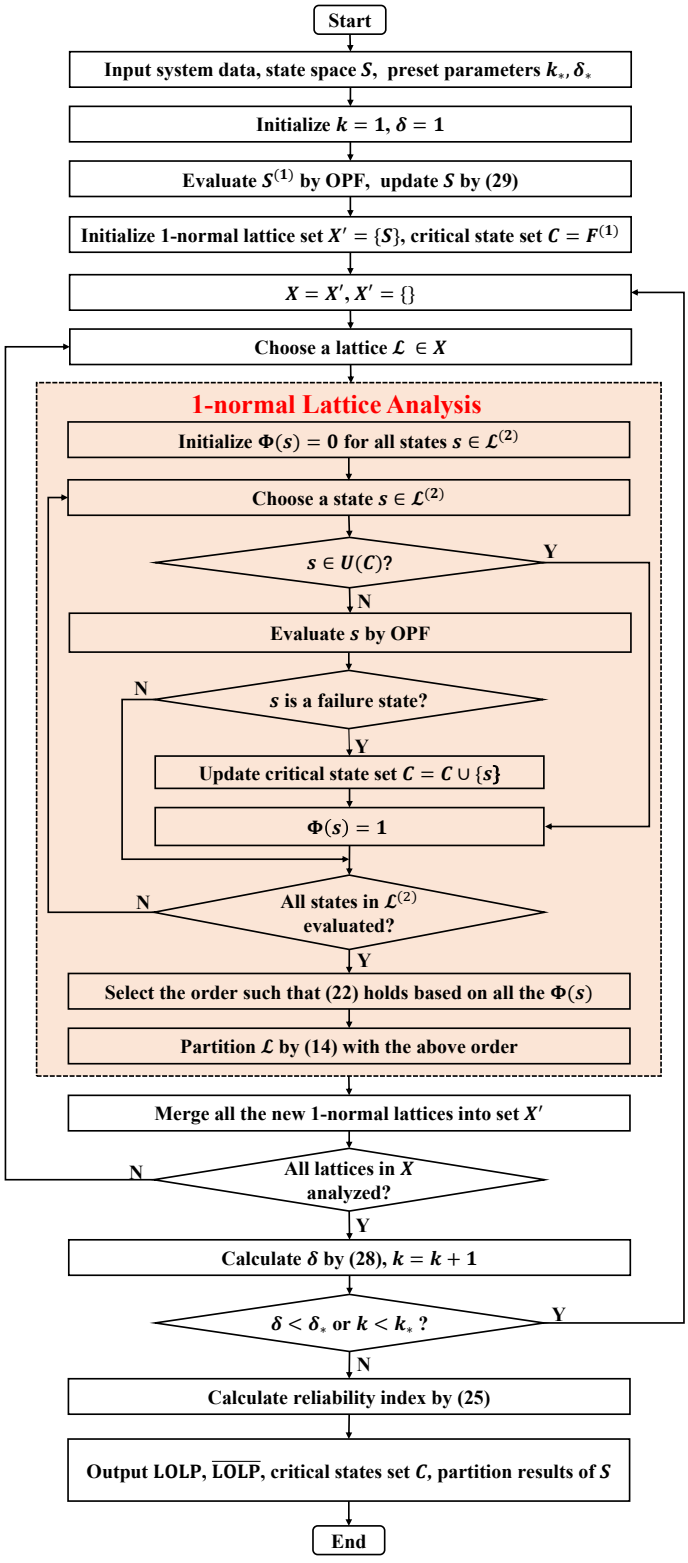

Figure 5. The overall process of the proposed method.

Note: The critical system state set C is updated in the 1-normal lattice analysis module, and partition results of S are derived from accumulating this module's lattice partition outcomes per iteration.

Step 1: Input system data, system state space S, preset parameters including k_* (maximum state search level), δ_* (minimal gap between the upper and lower bounds of the LOLP). Initialize $k = 1$, $\delta = 1$.

Step 2: Evaluate all the states in $S^{(1)}$ by OPF, update S to a 1-normal lattice by (29) based on the evaluation results.

Step 3: Initialize 1-normal lattice set $X^{'} = \{S\}$, critical state set $C = F^{(1)}$.

Step 4: $X = X^{'}$, $X^{'} = \{\}$.

Step 5: Choose a lattice $\mathcal{L} \in X$, apply Algorithm 1 to $\mathcal{L}$ as follows:

1. Initialize $\Phi(s) = 0$ for all the states $s \in \mathcal{L}^{(2)}$.
2. Choose an unevaluated 2-level state $s \in \mathcal{L}^{(2)}$.
3. Check if $s \in U(C)$, if so, s is evaluated as a failure state and set $\Phi(s) = 1$, go to Step 5.5; otherwise, go to Step 5.4.
4. Evaluate s by OPF. Check if s is a failure state, if so, s is identified as a critical state, set $\Phi(s) = 1$, and update critical state set $C = C \cup \{s\}$.
5. Check if all the states in $\mathcal{L}^{(2)}$ are evaluated, if not, go to Step 5.2.
6. Select order such that (22) holds with the results of all the $\Phi(s)$.
7. Partition $\mathcal{L}$ by (14) with the above order, obtain new 1-normal lattices.

Step 6: Merge all the new 1-normal lattices partitioned out in Step 5 into set $X^{'}$.

Step 7: Check if all the lattices $\mathcal{L} \in X$ are analyzed, if not, go to Step 5.

Step 8: Calculate δ by (28), $k = k + 1$.

Step 9: Check if $\delta < \delta_*$ or $k < k_*$, if so, go to Step 4.

Step 10: Calculate reliability index LOLP by (25).

Step 11: Output LOLP, $\overline{\text{LOLP}}$, critical states set C, partition results of S.

A few remarks:

- Simple states comparisions are needed when checking if $s \in U(C)$ in Step 5.3. This is the main computational burden in this method except for OPF calculations.
- All states in $F^{(1)}$ are critical states, as they constitute failure states with no failure states strictly smaller than themselves. Consequently, the critical state set C can be initialized as $F^{(1)}$ in Step 3.
- Each time the analysis of all lattices in X is completed, it means that the evaluation of all states at a certain level has been finished, so the approach actually proceeds level by level.

4.5. A 5-component system example

As an example, the approach is run on the synthetic 5-component system shown in Figure 3(c). Twelve OPF calculations are performed on the states represented by solid red and green circles, and the following information can be obtained.

The critical states are represented by solid red circles, and the set of critical states is:

$$C = \{\{1\}, \{2, 3\}, \{3, 4\}, \{2, 4, 5\}\}$$

The state space $\mathcal{L}$ can be partitioned into four failure lattices and four normal lattices, one of which is a 1-state lattice:

$$\begin{aligned}\mathcal{L} = {} & [\{1\}, \{1, 2, 3, 4, 5\}] \cup [\{2, 3\}, \{2, 3, 4, 5\}] \cup [\{3, 4\}, \{3, 4, 5\}] \cup [\{2, 4, 5\}, \{2, 4, 5\}] \\ & \cup [\{2, 4\}, \{2, 4\}] \cup [\{2\}, \{2, 5\}] \cup [\{3\}, \{3, 5\}] \cup [\{\}, \{4, 5\}]\end{aligned}$$

The LOLP index can be calculated analytically:

$$\text{LOLP} = P([\{1\},\{1,2,3,4,5\}]) + P([\{2,3\},\{2,3,4,5\}]) + P([\{3,4\},\{3,4,5\}]) + P(\{2,4,5\})$$

In the above example, the minimum states of failure lattices are all critical states. However, this is not a common scenario. More often, some failure lattices have minimal elements that are not critical states themselves but are greater than a certain critical state. Regardless of the scenario, the failure probability contributed by these failure lattices to the reliability index is essentially derived from certain critical states. In fact, the contribution of a critical state to the reliability index is actually the sum of the probabilities of all failure lattices it covers, which is significantly greater than the failure probability it contributes on its own.

It is noted that although all identified critical states carry a certain level of high risk, in the proposed method of this paper, some high-risk states may be covered by critical states and thus fail to be identified. If the risk coefficient is defined as the product of the load curtailment and probability of a state, $\{1,4\}$ or $\{1,5\}$ may be higher-risk states than $\{2,4,5\}$, and they may remain unidentified because they are not critical states. However, this will not cause misjudgment of localized risks since their impacts are all encompassed by the critical state $\{1\}$. Specifically, the load curtailment and risk contribution of these unrecognized high-risk states are fully reflected in the critical state that covers them, which means the localized risk evaluation results will not be biased.

4.6. Theoretical properties and complexity analysis

We now establish three key theoretical results for the LPCSI method: completeness of critical state identification (Theorem 4.1), existence of a finite maximum critical level (Theorem 4.2), and computational complexity characterization (Theorem 4.3).

Theorem 4.1 (Completeness)**.** *The LPCSI method can completely identify all critical states with a level of no more than k.*

Proof. We prove by induction on k that all states with level $\leq k$ are correctly classified.

Base case ($k = 1$): Preprocessing evaluates all 1-level states via OPF, identifying 1-level critical states as the 1-level failure states directly.

Inductive step: When $k = m$, assuming all states with level $\leq m$ are completely identified, then after the m-th round of partitioning, states with level $m + 1$ are evaluated as 2-level states of respective 1-normal lattices. Consider any 1-normal lattice $\mathcal{L}$ processed in round $m + 1$. By Theorem 3.2 and Corollary 3.2 , $\mathcal{L}$ is partitioned into:

$$\mathcal{L} = \mathcal{N}_{normal} \cup \left(\bigcup_i \mathcal{F}_i\right) \cup \left(\bigcup_j \mathcal{N}_{1,j}\right) \tag{30}$$

where $\mathcal{N}_{normal}$ is the normal lattice, $\mathcal{F}_i$ are failure lattices, and $\mathcal{N}_{1,j}$ are new 1-normal lattices. This partition forms a disjoint cover, and when the recursion depth is limited to k, it exactly traverses all states with a level of no more than k. For the partitioned states:

- Normal lattice $\mathcal{N}_{normal}$: all states satisfy $\Phi(s) = 0$, hence they are non-critical;

- Failure lattices $\mathcal{F}_i = [\underline{s}_i, \overline{s}_i]$: The minimum element $\underline{s}_i$ (a 2-level state in $\mathcal{L}$) is identified as a critical state or not in Step 3 of Algorithm 1; by Proposition 2.2, $\forall s \in \mathcal{F}_i \setminus \{\underline{s}_i\}$, $\Phi(s) = 1$ with failure subset state $\underline{s}_i$, hence $s \notin C$;

- 1-normal lattices $\mathcal{N}_{1,j}$: Preserved for the next iteration, whose 2-level states (m + 2-level states of S) will be evaluated in subsequent iterations.

Thus states with level $m+1$ are either identified as critical (minimum elements $\underline{s}_i$ of some failure lattices) or correctly classified as non-critical. The partition ensures disjoint coverage, guaranteeing no state is missed or double-counted. By induction, this holds for all levels up to any finite k, completing the proof. □

Theorem 4.2 (Existence of the maximum critical state level)**.** *Let S be the n-component system state space. There exists a finite integer*

$$k_{\max} = \min\left\{k \in \mathbb{N}^+ \,\middle|\, \forall s \in S^{(k)},\ s \text{ is a failure state}\right\} \tag{31}$$

such that all critical states $s \in C$ satisfy $\rho(s) \le k_{\max}$.

Proof. By the finiteness of the state space ($|S| = 2^n$) and system coherence, all states at sufficiently high levels must be failures, ensuring the existence and finiteness of $k_{\max}$.

For any s' with $\rho(s') > k_{\max}$, there exists a state $s \in S^{(k_{\max})}$ such that $s < s'$. By definition, $\Phi(s) = 1$ for all $s \in S^{(k_{\max})}$. By Proposition 2.2, $\Phi(s') = 1$. By the definition of a critical state, s' is not a critical state. Therefore, no critical states exist above level $k_{\max}$, implying $\rho(s) \le k_{\max}$ for all $s \in C$. □

Remark 1. Note that this $k_{\max}$ provides an upper bound, while the actual maximum critical state level may be strictly smaller.

Theorem 4.3 (Computational complexity)**.** *Let n be the system dimension,x the time complexity of the LPCSI algorithm is:*

$$T(n) = O\left(\sum_{k=1}^{k_{\max}} \left[\binom{n}{k} - g_k\right] \cdot \left[\rho_k T_{\mathrm{OPF}} + T_{\mathrm{comp}}\right] + m \cdot n^2\right) \tag{32}$$

where k_{max} is the maximal level of critical states, g_k is the number of states at level k belonging to failure lattices (covered by lattice partitioning and requiring no evaluation), $\rho_k \in (0,1)$ is the proportion of states requiring OPF evaluation after state comparison, T_{OPF} is the complexity of solving the optimal power flow problem for a given state, $T_{\mathrm{comp}} = O(|C| \cdot k)$ is the complexity of the state comparison for a level-k state, and $m = \sum_{k=1}^{k_{\max}} m_k$ is the total number of explicitly identified failure states triggering lattice partitioning.

Proof. The algorithm complexity majorly comprises two components:

(1) Explicit state evaluation: At level k, the total number of states is $\binom{n}{k}$, among which g_k states are already covered by previously identified failure lattices (as non-minimal elements) and require no evaluation. The remaining $\binom{n}{k} - g_k$ states are processed explicitly:

- All undergo state comparison (checking if they are covered by $U(C)$);

• A fraction ρ_k of them require OPF evaluation after comparison.

The total evaluation complexity is:

$$O\left(\sum_{k=1}^{k_{\max}}\left[\binom{n}{k}-g_k\right]\cdot\left[\rho_k T_{\mathrm{OPF}}+T_{\mathrm{comp}}\right]\right)$$

(2) Lattice partitioning: Only $m_k < \binom{n}{k} - g_k$ explicitly identified failure states (via OPF or state comparison) at level k trigger lattice partitioning, each with complexity at most $O(n^2)$, yielding total complexity $O(m \cdot n^2)$, where $m = \sum_{k=1}^{k_{\max}} m_k$.

Summing (1) and (2) yields the total time complexity. □

Remark 2. Note that $T_{\mathrm{OPF}} \gg T_{\mathrm{comp}}$ in practice, as solving OPF involves solving a nonlinear optimization problem while state comparison only involves simple set operations. Due to lattice partitioning, g_k grows rapidly with k, satisfying $\binom{n}{k} - g_k < \binom{n}{k}$. Combined with $\rho_k < 1$, we have:

$$\sum_{k=1}^{k_{\max}}\rho_k\left[\binom{n}{k}-g_k\right]<\sum_{k=1}^{k_{\max}}\binom{n}{k}\ll 2^n$$

In practical power systems, $k_{\max} < n/2$ and $g_k \sim O(\binom{n}{k-1})$ (a failure state generates numerous higher-level states in failure lattices), yielding near-polynomial complexity.

5. Numerical experiments

The proposed LPCSI method for critical states identification and system reliability evaluation was tested on two power systems: a 6-bus system RBTS and a 24-bus system RTS79. The identified critical states for both systems will be presented in the order of their levels, along with the proportion of each level's critical states relative to the total number of states at that level. The reliability assessment results, specifically the loss of load probability (LOLP), were compared among the sequential enumeration (SE) method, Monte Carlo simulation (MCS) method, and LPCSI method. We set different values for each stop criterion to compare efficiency and accuracy of the three methods. The experiments were conducted on a standard PC equipped with an Intel(R) Core(TM) i9-14900K CPU at 3.20 GHz and 32GB RAM, using MATLAB R2020b with the Yalmip and Gurobi toolboxes.

5.1. Results on the RBTS system

The RBTS system is a small-scale composite system with 11 generations, 9 transmission lines, and 6 buses. The total installed capacity of generations is 240 MW, with an annual peak load of 185MW.

5.1.1. Results of critical states

For the entire system, the LPCSI method partitioned out a total of 2,896 failure lattices from the state space and identifies 62 critical states. These 62 critical states correspond to the minimal elements of 62 distinct failure lattices among the 2,896 lattices. The identified critical states are distributed across levels one to five, as shown in Table 1. The table also lists the number of critical states at each level and

the proportion of these critical states relative to the total number of system states at each level. The proportion of critical states at level 2 is the highest, which demonstrates that identifying critical states in the 2-level state space of every lattice is crucial and effective.

Table 1. Critical states (RBTS).

Level	Number (Proportion)	Critical State
1	1 (5%)	{20}
2	19 (10%)	{1,2},{1,4},{1,7},{1,8},{1,9},{1,10},{1,11},{2,4},{2,7},{2,8} {2,9},{2,10},{2,11},{4,7},{7,8},{7,9},{7,10},{7,11},{16,19}
2	15 (1.32%)	{4,8,9},{4,8,10},{4,8,11},{4,9,10},{4,9,11},{4,10,11}, {8,9,10},{8,9,11},{8,10,11},{9,10,11},{12,13,17}, {12,14,17},{12,17,18},{13,14,18},{14,15,19}
4	10 (0.21%)	{1,3,5,6},{1,14,15,16},{2,3,5,6},{2,14,15,16},{3,5,6,7} {7,14,15,16},{12,15,16,17},{12,15,17,19}, {13,15,16,18},{13,15,18,19}
5	17 (0.11%)	{3,4,5,6,8},{3,4,5,6,9},{3,4,5,6,10},{3,4,5,6,11},{3,4,14,15,16}, {3,5,6,8,9},{3,5,6,8,10},{3,5,6,8,11},{3,5,6,9,10},{3,5,6,9,11} {3,5,6,10,11},{8,9,14,15,16},{8,10,14,15,16},{8,11,14,15,16}, {9,10,14,15,16},{9,11,14,15,16}{10,11,14,15,16}

Table 2. Indices of critical states (RBTS).

Critical State	Level	Risk	ΔLOLP		LOLP (%)	OPF Number
			Value (%)	Proportion (%)		
{20}	1	1.81e-2	0.114155	12.047	0.1141553	20
{1, 2}	2	1.90e-2	0.089897	9.488	0.2040525	21
{1, 4}	2	3.14e-3	0.072667	7.669	0.2767195	23
			⋮			
{16, 19}	2	4.14e-5	1.291e-4	0.013	0.9432331	188
{4, 8, 9}	3	2.36e-5	5.181e-4	0.055	0.9437511	559
			⋮			
{14, 15, 19}	3	8.91e-8	7.359e-7	7.82e-5	0.9475025	892
{1, 14, 15, 16}	4	2.76e-9	1.942e-8	2.13e-6	0.9475025	930
			⋮			
{13, 15, 18, 19}	4	1.36e-9	4.176e-9	4.41e-7	0.9475164	2901
{3, 4, 14, 15, 16}	5	1.55e-11	3.42e-10	3.61e-8	0.9475164	3677
			⋮			
{3, 5, 6, 10, 11}	5	1.91e-9	3.921e-8	4.14e-6	0.9475169	4712

As shown in Table 2, some of the critical states and their associated data are listed in the order they were identified. The risk of a state was the product of the probability and load shedding of the state according to [20], ΔLOLP of a state represents its total contribution to the LOLP while ΔLOLP

Proportion represents the proportion of ΔLOLP in the final LOLP. ΔLOLP of these critical states generally shows a downward trend in descending order. It can be observed that the order in which the critical states are identified by the LPCSI method often reflects their risk levels and contributions to the LOLP. Specifically, the critical states identified first tend to be those with higher risk and greater ΔLOLP. Therefore, this test system demonstrates that the proposed method can identify critical states in a reasonable order. However, there are some exceptions where the order deviates slightly from this trend; this is because the order of 1-level states in a 1-normal lattice to be partitioned is not the optimal choice and there is still room for improvement.

5.1.2. Results of the reliability assessment

For comparison, the SE method traversed all possible system states of the entire system, and its assessment results serve as the baseline for calculating the accuracy of the other two methods. The stop criterion for the MCS method is set to a coefficient of variation of 0.01.

As shown in Table 3, the index yielded by SE and LPCSI are exactly the same, so the error of the LPCSI is 0%. However, error of MCS is 0.26%. In addition, it cost the SE method about 65,734 seconds to reach the analytical value. Such precision can be reached by LPCSI within 887 seconds, which is almost 100 times faster than SE. MCS cannot reach the precision even with more than 1000 seconds, which is slower and less efficiency.

Table 3. Results of the three assessment methods (RBTS).

Method	LOLP		OPF	CPU
	Value (%)	Error (%)	Number	Time (s)
SE	0.9475169361176	——	1048576	65734
MCS	0.9053411493810	0.2648	19882	1200
LPCSI	0.9475169361176	0.0000	15335	887

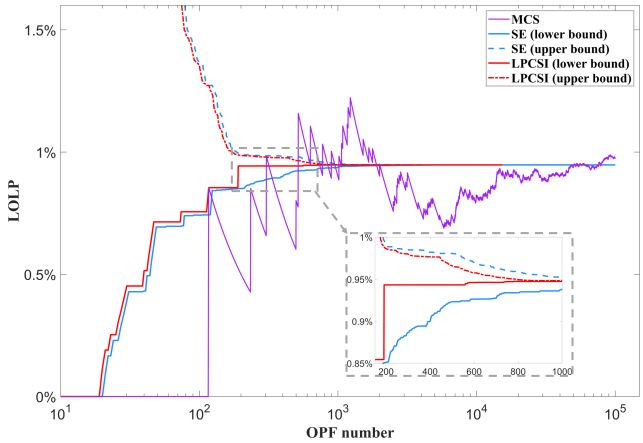

Figure 6. Results of the three assessment methods (RBTS).

Convergence curves based on the OPF number are shown in Figure 6, indicating that the upper and lower bounds of LPCSI converge faster than those of SE, and the convergence of the MCS method is

not only slow but also results in inaccurate values. After the same number of OPF calculations, results yielded by LPCSI are more accurate. Specifically, the error in the LOLP calculated by the LPCSI method is approximately 0.45% after 200 OPF calculations, which falls within an acceptable range. This stems from the fact that, within 200 OPF calculations, the LPCSI method has already evaluated all states at levels 1 and 2, and numerous critical states have been identified. These states contribute significantly to the LOLP by encompassing the probabilities of a substantial portion of failure lattices.In contrast, the SE method requires more OPF calculations to achieve a similar level of precision.

Furthermore, the preset gap between the upper and lower bounds of the LOLP, δ_*, also significantly impacts the performance of the LPCSI method: a smaller δ_* requires more state evaluations, which can be observed from Table 4. For example, achieving $\delta < 10^{-10}$ took 580 seconds and 9879 OPF calculations, and the relative error was reduced to $1.57 \times 10^{-7}\%$. In contrast, SE required nearly ten times more evaluations and time to reach the same δ_*, and still resulted in a larger relative error.

Table 4. The impact of different stop criterion (gap) on accuracy and efficiency (RBTS).

δ_*	Method	LOLP		$\overline{\text{LOLP}}$ (%)	OPF	CPU
		Value (%)	Error (%)		Number	Time (s)
10^{-4}	SE	0.941726	0.61120	0.951684	1077	70
	LPCSI	0.946215	0.13737	0.956108	627	54
10^{-6}	SE	0.947425	0.00975	0.947525	8512	454
	LPCSI	0.947502	0.001559	0.947602	2382	163
10^{-8}	SE	0.947516	1.01e-04	0.947517	36550	1892
	LPCSI	0.947517	9.94e-06	0.947518	5760	349
10^{-10}	SE	0.947517	1.04e-06	0.947517	99395	5076
	LPCSI	0.947517	1.57e-07	0.947517	9879	580

Table 5. The impact of different stop criterion (level) on accuracy and efficiency (RBTS).

k_*	Method	LOLP		OPF Number
		Value (%)	Error (%)	
2	SE	0.852125	10.0676	211
	LPCSI	0.943224	0.4531	191
3	SE	0.942294	0.5513	1351
	LPCSI	0.947385	0.0139	899
4	SE	0.947336	0.0191	6196
	LPCSI	0.947516	1.53e-04	2905
		⋮		
9	SE	0.947517	1.87e-10	431910
	LPCSI	0.947517	0.0000	15335

As shown in Table 5, k_* can also affect the performance of LPCSI and SE. A larger k_* indicates a broader search range and higher precision, but at the cost of increased computational time. For the same k_* value, the index error obtained by the LPCSI method is consistently 1–2 orders of magnitude smaller than that of the SE method, with less OPF calculations. For example, after completing the second-level

state evaluation, the LOLP error of the LPCSI method drops sharply to 0.45%, while the error of the conventional SE method remains around 10%, with the difference between the two errors exceeding an order of magnitude. However, SE needs to evaluate states up to the first three levels to reach the same precision, as can also be observed in Figure 7, which presents the cumulative contribution to the LOLP from each state level. Moreover, it is evident that the indices calculated by LPCSI converge to the true values upon evaluating all states up to the ninth level. This arises because the critical states at this round cover all failure lattices, thereby accounting for the entire failure state space.

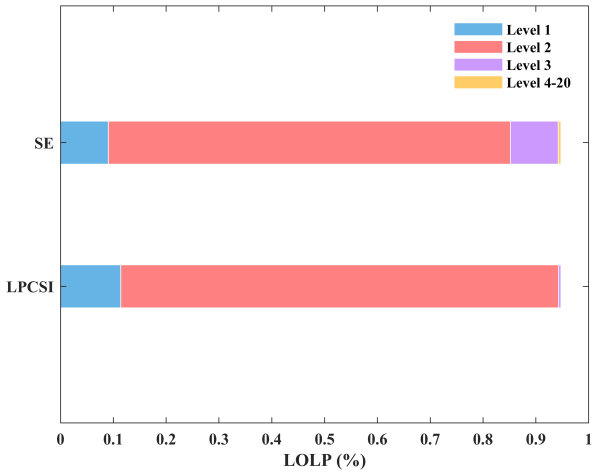

Figure 7. LOLP contribution of each level (RBTS).

5.2. Results on the RTS79 system

In this system, there are 24 buses, 32 generators, 38 transmission lines. The total installed capacity is 3405 MW, with an annual peak load of 2850 MW.

5.2.1. Results of critical states

With k_* is set as 4, the proposed method partitioned out 4787 failure lattices from the the state space of the RTS79 system and identified 2785 critical states of the first four levels. Some of the critical states of the first four levels are shown in Table 6 with the order they were identified, and there are no 1-level critical states in this state space since all the 1-level states are normal. The percentages in parentheses indicate the proportion of these numbers relative to the total number of system states of that level. For example, the number of 2-level critical states is 15, accounting for 0.62% of the total number of 2-level states. Similar to Table 2, Table 7 lists some critical states and their related indices, where the order in which these critical states were identified generally follows the order of their risk or ΔLOLP, from highest to lowest.

Table 6. Critical states (RTS79).

Level	Number (Proportion)	Critical State
2	15 (0.62%)	{12,22},{12,23},{13,22},{13,23},{14,22},{14,23},{22,23}, {22,32},{22,43},{23,32},{23,43},{35,41},{36,40},{37,42},{51,55}
3	383 (0.7%)	{1,20,22},{1,21,22},{1,22,30},{1,22,31},{2,20,22},{2,21,22}, {2,22,30},{2,22,31},{3,9,22},{3,10,22},{3,11,22},{3,20,22} ⋮ {55,59,61},{56,59,60}{57,58,60},{61,66,67},{61,68,69}
4	2477 (0.27%)	{20,22,44,45},{21,22,44,45},{22,30,44,45},{22,31,44,45}, {1,9,22,24},{1,9,22,25},{1,9,22,26},{1,9,22,27},{1,9,22,28}, ⋮ {56,57,58,59},{56,59,62,63},{57,58,62,63},{66,67,68,69}

Table 7. Indices of critical states (RTS79).

Critical State	Level	Risk	ΔLOLP		LOLP (%)	OPF Number
			Value (%)	proportion (%)		
{12, 22}	2	6.95e-02	0.600000	7.130705	0.600000	784
{12, 23}	2	6.95e-02	0.528000	6.275020	1.128000	785
{13, 22}	2	6.95e-02	0.570000	6.774169	1.698000	841
			⋮			
{51, 55}	2	1.04e-05	2.157e-05	2.563e-04	5.906683	2299
{1, 20, 22}	3	2.91e-03	0.033307	0.395836	5.939990	2501
			⋮			
{61, 68, 69}	3	5.54e-09	4.531e-09	5.385e-08	8.282226	56149
{20, 22, 44, 45}	4	1.32e-09	3.379e-08	4.016e-07	8.282226	56548
			⋮			
{66, 67, 68, 69}	4	1.22e-12	9.573e-13	1.142e-11	8.414316	921223

5.2.2. Results of the reliability Assessment

The LPCSI method was applied to the system up to the fourth level to test its accuracy and efficiency in reliability assessment. It was compared with SE and MCS, as shown in Table 8 and Figure 8. SE enumerated all the states of the first four levels, and the stop criterion for MCS was set as a preset total sampled state number of 1,000,000 (finally reaching a variance of 0.004546).

The LOLP ($\underline{\text{LOLP}}$) and $\overline{\text{LOLP}}$ of the RTS79 system generated by the LPCSI method reached approximately 8.41% and 8.75%, respectively, with only a 0.34% gap between them. In contrast, the upper and lower bounds of the LOLP generated by SE exhibited a gap of approximately 1.13%, which is relatively large. Moreover, the LPCSI method computes LOLP values in a monotonically increasing manner, whereas the MCS method exhibits inherent instability. The LOLP value obtained by LPCSI exceeds that calculated by the MCS method (8.33%), indicating that LPCSI yields a more accurate result.

Additionally, the LPCSI method achieved these results with the fewest OPF calculations (921,157) among the three methods, which demonstrates that LPCSI requires the least computational effort and provides the most accurate index. As shown in Figure 8, the LOLP upper and lower bounds curves generated by the LPCSI method converge more rapidly than those produced by the SE method and MCS method.

Table 8. Results of the three assessment methods (RTS79).

Method	LOLP (%)	$\overline{\text{LOLP}}$ (%)	OPF Number	CPU Time (s)
SE	7.620934	8.753119	974120	60214
MCS	8.333100	——	1000000	60797
LPCSI	8.414316	8.753119	921157	57737

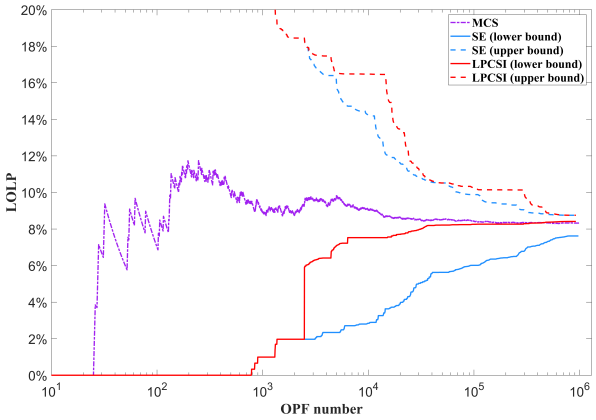

Figure 8. Results of the three assessment methods (RTS79).

As shown in Table 9, under the same δ_*, SE always requires a higher number of OPF calculations and more time compared to LPCSI. Additionally, SE can only achieve a maximum gap of 0.02 between the upper and lower bounds, while LPCSI can achieve a gap that is an order of magnitude smaller (e.g., 0.004). Note that while δ is typically of order 10^{-p} ($p \geq 2$) in practice, we intentionally employ 0.02 and 0.004 here to ensure a fair comparison, thereby also revealing SE's inability to achieve the tighter gap attained by LPCSI.

Table 9. The impact of different stop criterion (gap) on accuracy and efficiency (RTS79).

δ_*	Method	LOLP (%)	OPF Number	CPU Time (s)
0.1	SE	0.314348	12370	701
	LPCSI	6.871609	4680	428
0.02	SE	6.938624	309905	17876
	LPCSI	8.259270	103519	8384
0.01	LPCSI	8.324125	352881	23340
0.004	LPCSI	8.395841	613184	38677

The higher k_* is set, the more accurate the index becomes. As shown in Table 10, LPCSI always achieves a better index than SE at the same Level. When $k_* = 2$ and 3, although the difference of the

number of OPF calculations of the two methods is not significant, the LOLP obtained by LPCSI is more accurate than that of SE. This is attributable to the fact that LPCSI encompasses the probabilities of failure lattices generated by critical states. As shown in Figure 9, the LOLP obtained by the LPCSI method after completing the first two levels of states evaluation can cover those that the SE method only achieves after finishing the first three levels of states evaluations.

Table 10. The impact of different stop criterion (level) on accuracy and efficiency (RTS79).

k_*	Method	LOLP (%)	OPF Number
2	SE	1.969654	2485
	LPCSI	5.906663	2485
3	SE	5.629576	57225
	LPCSI	8.216603	56235
4	SE	7.620934	974120
	LPCSI	8.414316	921227

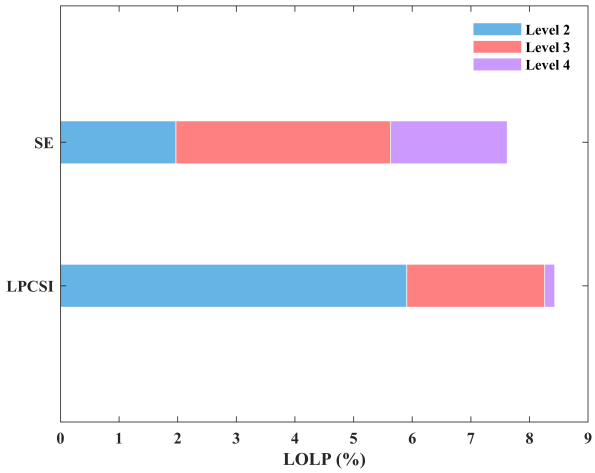

Figure 9. LOLP contribution of each level (RTS79).

5.3. Computational performance and scalability analysis

Table 11 presents the CPU time breakdown for both systems. The OPF solution dominates the total computational cost, accounting for 98.4% for RBTS and 87.5% for RTS79, while the overhead of lattice partitioning and state comparison increases with system size (8.9% for RTS79 in total, with absolute values increasing by approximately 68 times). However, this overhead remains small compared to the OPF time saved by the proposed method. Thus, the time saved from reduced OPF evaluations far exceeds the extra overhead of non-OPF tasks, when achieving the same level of reliability index accuracy.

Table 11. CPU time breakdown (s).

System	OPF	State Comparison	Lattice Partition	Component Ordering	Total
RBTS	872.9 (98.4%)	7.2 (0.8%)	4.1 (0.5%)	1.7 (0.2%)	887.5
RTS79	50546.4 (87.5%)	4935.7 (8.5%)	150.9 (0.3%)	61.9 (0.1%)	57737.3

To complement the theoretical analysis, we present an empirical assessment based on the RBTS and RTS79 test systems as follows. The RBTS system has dimensions $n = 20$ with $k_{\max} = 5$, and the RTS79 system has $n = 70$ with an empirically observed $k_{\max}$ below 10.

The complexity growth from RBTS to RTS79 aligns with Theorem 4.3: the effective evaluated states scale with $\sum_{k=1}^{k_{\max}} [\binom{n}{k} - g_k]$ rather than 2^n. Empirically, increasing n from 20 to 70 (a 3.5-fold increase) while $k_{\max}$ grows from 5 to below 10 results in evaluation growth from 1.5×10^4 to 10^6 (roughly 60-fold), suggesting a superlinear but subexponential dependence on n when $k_{\max}$ is constrained.

We acknowledge that approximately 10^6 OPF evaluations for RTS79 indicates substantial computational demand, and the absolute cost may become prohibitive for systems with $n > 100$. The OPF solution time dominates the total computational cost, presenting a bottleneck for further scaling. To address this, we have identified a promising direction for future work: leveraging the characteristics of critical system states and similar states to introduce an acceleration strategy that can reduce the number of required OPF evaluations and improve overall efficiency on larger systems.

6. Conclusion

This paper applied a lattice structure to represent and partition the system's state space (enabling failure state extension and high-level impacts incorporation) and proposed a recursive method (LPCSI) to identify critical states and accelerate reliability assessment. Notably, the method also supports risk monitoring: under peak load conditions or following equipment contingencies, it identifies high-risk states and outputs updated indices to inform operational decisions. However, limitations exist: 1) Index growth and critical state identification speed depend on lattice partitioning order and selection criteria, leaving room for optimization; 2) it may face the curse of dimensionality in very large systems, as more components cause exponential state space expansion, increasing computational burden and limiting scalability. Future research will optimize partitioning order, combined with dimensionality reduction techniques, and exploit similarities among critical states to reduce OPF computational burden, thereby adapting the method to large systems and enhancing its practical value.

Author contributions

Feiyu Chen: Conceptualization, Supervision, Funding acquisition. Han Hu: Writing—original draft, Investigation, Data curation (graduate student, main drafter of the paper). Wenjie Wan: Methodology, Validation. Hongyu Zhang: Formal analysis, Visualization. Xiaoyu Liu: Resources, Writing—review and editing, Project administration. Bo Yu: Supervision, Writing—review and editing. Kequan Zhao: Conceptualization, Methodology.

Acknowledgments

The authors would like to express their gratitude to all individuals who contributed to the completion of this study. This work was financially supported by the Key Technology Research and Development Program of China (Award Number: 2023YFA1011302). The authors also appreciate the guidance and assistance from their academic colleagues during the research process.

Conflict of interest

The authors declare no conflict of interest. All authors have no relevant financial or non-financial interests to disclose that could be perceived as affecting the objectivity of this work.

Use of Generative-AI tools declaration

The authors declare that they did not utilize any artificial intelligence (AI) tools in the creation of this article.

References

1. C. Y. Zhao, H. B. Liu, X. Q. Qu, M. X. Liu, R. T. Tang, A. K. Xie, Reliability analysis of floating offshore wind turbine generator based on failure prediction and preventive maintenance, *Ocean Eng.*, **288** (2023), 116089. https://doi.org/10.1016/j.oceaneng.2023.116089
2. H. B. Liu, C. Y. Zhao, G. Ma, L. X, He, L. P. Sun, H. Li, Reliability assessment of a floating offshore wind turbine mooring system based on the tlbo algorithm, *Appl. Ocean Res.*, **124** (2022), 103211. https://doi.org/10.1016/j.apor.2022.103211
3. H. J. Yang, Y. X. Yue, J. Ma, D. B. Zhang, X. J. Qi, Reliability enhancement method for distribution system using a network cooperation recovery optimization technique, *Eng. Sci. Technol. Int. J.*, **74** (2026), 102285. https://doi.org/10.1016/j.jestch.2026.102285
4. Y. Kou, Z. H. Bie, G. F. Li, F. Liu, J. F. Jiang, Reliability evaluation of multi-agent integrated energy systems with fully distributed communication, *Energy*, **224** (2021), 120123. https://doi.org/10.1016/j.energy.2021.120123
5. D. M. Zhang, G. F. Li, Z. H. Bie, K. J. Fan, An analytical method for reliability evaluation of power distribution system with time-varying failure rates, *Reliab. Eng. Syst. Saf.*, **250** (2024), 110290. https://doi.org/10.1016/j.ress.2024.110290
6. B. Lami, K. Bhattacharya, Identification of critical components of composite power systems using minimal cut sets, *ISGT 2015*, 2015, 1–5. https://doi.org/10.1109/ISGT.2015.7131786
7. R. Billinton, W. Li, *Reliability assessment of electric power systems using monte carlo methods,* Springer New York, 1994. https://doi.org/10.1007/978-1-4899-1346-3
8. J. W. Lee, S. W. Kim, Reliability-centered maintenance strategy for redundant power networks using the cut set method, *J. Electr. Eng. Technol.*, **17** (2022), 1615–1621. https://doi.org/10.1007/s42835-022-01031-4
9. N. K. Jyotish, L. K. Singh, C. Kumar, P. Singh, Reliability and performance measurement of safety-critical systems based on petri nets: A case study of nuclear power plant, *IEEE Trans. Reliab.*, **72** (2023), 1523–1539. https://doi.org/10.1109/TR.2023.3244365
10. T. B. Kumar, O. C. Sekhar, M. Ramamoorty, Composite power system reliability evaluation using modified minimal cut set approach, *Alex. Eng. J.*, **57** (2018), 2521–2528. https://doi.org/10.1016/j.aej.2017.09.008
11. Z. F. Zhou, Z. Gong, B. Zeng, L. P. He, D. Ling, Reliability analysis of distribution system based on the minimum cut-set method, *ICQR2MSE*, 2012, 112–116. https://doi.org/10.1109/ICQR2MSE.2012.6246198

12. R. Billinton, *Power system reliability evaluation,* Springer New York, 1970.
13. J. B. Dugan, S. J. Bavuso, M. A. Boyd, Dynamic fault-tree models for fault-tolerant computer systems, *IEEE Trans. Reliab.*, **41** (1992), 363–377. https://doi.org/10.1109/24.159800
14. L. R. Ford, D. R. Fulkerson, Maximal flow through a network, *Can. J. Math.*, **8** (1956), 399–404. https://doi.org/10.4153/CJM-1956-045-5
15. D. R. Ford, D. R. Fulkerson, *Flows in networks*, Princeton University Press, 2010. https://doi.org/10.1007/978-1-84800-998-1_4
16. R. Billinton, R. N. Allan, *Reliability evaluation of engineering systems,* Springer, 1992. https://doi.org/10.1007/978-1-4899-0685-4
17. Y. Liu, C. Singh, Reliability evaluation of composite power systems using markov cut-set method, *IEEE Trans. Power Syst.*, **25** (2010), 777–785. https://doi.org/10.1109/TPWRS.2009.2033802
18. H. T. Liu, Y. Z. Sun, P. Wang, L. Cheng, L. Goel, A novel state selection technique for power system reliability evaluation, *Electr. Power Syst. Res.*, **78** (2008), 1019–1027. https://doi.org/10.1016/j.epsr.2007.08.002
19. Y. B. Jia, P. Wang, X. Q. Han, J. Y. Tian, C. Singh, A fast contingency screening technique for generation system reliability evaluation, *IEEE Trans. Power Syst.*, **28** (2013), 4127–4133. https://doi.org/10.1109/TPWRS.2013.2263534
20. T. Ding, C. Li, C. Yan, F. X. Li, A bi-level optimization model for risk assessment and contingency ranking in transmission system reliability evaluation, *IEEE Trans. Power Syst.*, **31** (2016), 1. https://doi.org/10.1109/TPWRS.2016.2637060
21. Y. B. Jia, Z. Yan, P. Wang, An improved state selection technique for power system reliability evaluation, in *IEEE Power Energy Soc. Gen. Meet.*, 2011, 1–6. https://doi.org/10.1109/PES.2011.6039271
22. D. Clancy, G. Gross, F. Wu, Probabilistic flows for reliability evaluation of multiarea power system interconnections, *Int. J. Electr. Power Energy Syst.*, **5** (1983), 101–114. https://doi.org/10.1016/0142-0615(83)90014-5
23. R. Billinton, W. Zhang, State extension in adequacy evaluation of composite power systems—concept and algorithm, *Electr. Power Syst. Res.*, **47** (1998), 189–195. https://doi.org/10.1016/S0378-7796(98)00064-9
24. R. Billinton, W. Zhang, State extension for adequacy evaluation of composite power systems-applications, *IEEE Trans. Power Syst.*, **15** (2000), 427–432. https://doi.org/10.1109/59.852155
25. K. Hou, H. J. Jia, X. D. Yu, L. W. Zhu, X. D. Xu, X. Li, An impact increments-based state enumeration reliability assessment approach and its application in transmission systems, *IEEE Power Energy Soc. Gen. Meet.*, 2016, 1–5. https://doi.org/10.1109/PESGM.2016.7741639
26. B. E. Sagan, Combinatorics: The art of counting, *American Mathematical Soc.,* 2020. https://doi.org/10.1090/gsm/210

AIMS Press